Catalyst-Directed Guidance of Sulfur-Substituted Enediolates to Stereoselective Carbon-Carbon Bond Formation with Aldehydes

Daisuke Uraguchi, Kohei Yamada, Makoto Sato, and Takashi Ooi

J. Am. Chem. Soc., **Just Accepted Manuscript** • DOI: 10.1021/jacs.7b12949 • Publication Date (Web): 04 Mar 2018

Catalyst-Directed Guidance of Sulfur-Substituted Enediolates to Stereoselective Carbon-Carbon Bond Formation with Aldehydes

Daisuke Uraguchi,[†] Kohei Yamada,[†] Makoto Sato,[‡] and Takashi Ooi*[†,‡]

[†]Institute of Transformative Bio-Molecules (WPI-ITbM) and Department of Molecular and Macromolecular Chemistry, Graduate School of Engineering, Nagoya University, Nagoya 464-8601, Japan.

[‡]CREST, Japan Science and Technology Agency (JST), Nagoya University, Nagoya 464-8601, Japan.

ABSTRACT: A highly chemo-, regio-, and stereoselective glycolate aldol reaction of sulfur-substituted enediolates with aldehydes was developed by employing a L-cyclohexylglycine-derived chiral iminophosphorane as a catalyst. The key for establishing this protocol is the distinct ability of the iminophosphorane catalyst to precisely direct the equilibrium mixture of the enediolates toward the intermolecular carbon-carbon bond formation with simultaneous yet rigorous control of relative and absolute stereochemistry. The critical importance of the cyclohexyl substituents on the catalyst backbone in dictating the reaction pathway and the stereochemical outcome was elucidated through an extensive quantum analysis by density functional theory calculations.

INTRODUCTION

Sulfur-substituted 1,2-enediolates are key intermediates in the first step of the glyoxalase pathway, an essential two-step detoxification of methylglyoxal and other reactive α-oxoaldehydes produced in the metabolism of living organisms. In this step, these glyoxals spontaneously react with the coenzyme glutathione to form the requisite hemithioacetals that undergo enantioselective isomerization to optically active α-hydroxy thioesters, wherein lactoylglutathione lyase (glyoxalase I) facilitates the facial- and regioselective protonation of the enediolate by transferring an internal proton from C1 to C2 of the hemithioacetal (Figure 1a).[1] Largely due to the synthetic importance of the resulting α-hydroxy thioesters as precursors of various chiral α-hydroxy carbonyl compounds, several small-molecule catalysts that mimic this enzymatic process have been introduced.[2] On the other hand, a mechanistically similar isomerization of *O*-acylated hemithioacetals **2**, readily accessible from the Pummerer reaction of β-keto sulfoxides, is a well-documented strategy for straightforward access to *O*-acylated α-hydroxy thioesters **3** (Figure 1b).[3–5] This transformation also involves a sulfur-substituted enediolate as a crucial intermediate and it exists as an equilibrium mixture of three types of enediolates. Upon considering their mutual interconversion via intramolecular acyl migration, the base-mediated isomerization can be understood as a consequence of the site-selective protonation of the enediolate. This outcome probably stems from the considerable pK_a difference between the α-protons of **2** and **3**, which makes the protonation leading to **3** irreversible, and the use of a chiral tertiary amine base as a catalyst has proven to be effective for controlling its absolute stereochemistry.[5c] Ironically, however, the inherent reactivity profile of the sulfur-substituted enediolates as ambident carbon nucleophiles

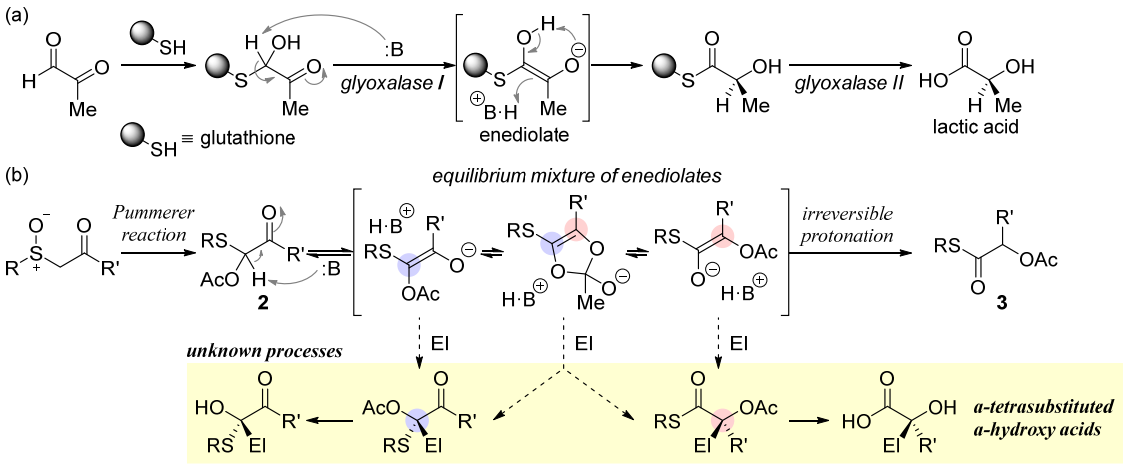

Figure 1. Isomerization of hemithioacetals to α-hydroxy acids via enediolate intermediates and potential intermolecular bond formations of the enediolate with an electrophile (El).

remains obscure within the protonation manifold. Moreover, the potential utility of the hemithioacetal isomerization as a means for catalytic generation and functionalization of highly basic enolates of carboxylic acid oxidation state has never been explored. In fact, despite significant mechanistic and synthetic relevance, the union of an enediolate and an external carbon or heteroatom electrophile into an α-tetrasubstituted α-hydroxy carbonyl entity is entirely unknown, and so are catalyst-controlled stereoselective systems. This deficiency is tightly associated with not only the ambiguity of the regioselectivity issue but also the stringent difficulty in promoting the intermolecular bond formation predominantly over facile protonation, while rigorously controlling the stereoselectivity. Herein, we disclose a catalyst-directed approach to address this challenging problem; that is, chiral iminophosphorane catalysts of type **1**,[6-12] upon deprotonation of **2**, precisely direct the corresponding sulfur-substituted enediolate toward aldolization with aldehydes with a high level of diastereo- and enantiocontrol, thereby revealing the intrinsic reactivity preference of the enediolates through the development of a novel protocol for the rapid assembly of chiral α,β-dihydroxycarboxylic acids bearing a fully substituted α-carbon stereocenter. The origin of the chemo-, regio-, and stereoselectivity observed in the present glycolate aldol reaction is elucidated based on the free-energy profile derived from the density functional theory (DFT) calculation.

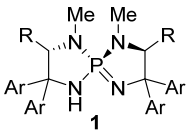

1

1a: R = ^{i}Pr, Ar = Ph
1b: R = Me, Ar = Ph
1c: R = ^{t}Bu, Ar = Ph
1d: R = (*S*)-^{s}Bu, Ar = Ph
1e: R = ^{c}Hex, Ar = Ph
1f: R = ^{c}Hex, Ar = 4-MeC_6H_4
1g: R = ^{c}Hex, Ar = 4-FC_6H_4

Figure 2. *P*-Spiro chiral iminophosphoranes.

RESULTS AND DISCUSSIONS

At the outset of our research, we selected racemic α-acetoxy-β-ketosulfide **2a** as a representative substrate and assessed the inherent reactivity of the enediolate generated from **2a** in the reaction with benzaldehyde (**4a**) by using a catalytic amount of common bases (10 mol%) in diethyl ether at −40 °C. With DBU as a catalyst, **2a** underwent quantitative isomerization to *O*-acetyl lactic acid thioester **3a**, indicating that C2-protonation of the intermediary enediolate occurred exclusively over the aldol coupling with **4a**. The use of a stronger base, KO^{t}Bu, allowed for the intervention of the aldol reaction followed by acyl migration to preferably afford a diastereomeric mixture of **5a** (dr = 2.1:1, 58% yield) likely due to the reluctant protonation by HO^{t}Bu; however, **3a** was also produced in 32% yield (Scheme 1). Notably, the regioisomeric aldol adduct **6** was not detected under these conditions, which would reflect the intrinsic difference in reactivity between the two nucleophilic sites of the enediolate.

Based on these observations, we set out to investigate the reaction under the influence of chiral iminophosphorane **1** in order to evaluate the possibility of simultaneously controlling reactivity and selectivity of the enediolate. In the initial attempt with L-valine-derived **1a**[13] as a catalyst under otherwise similar

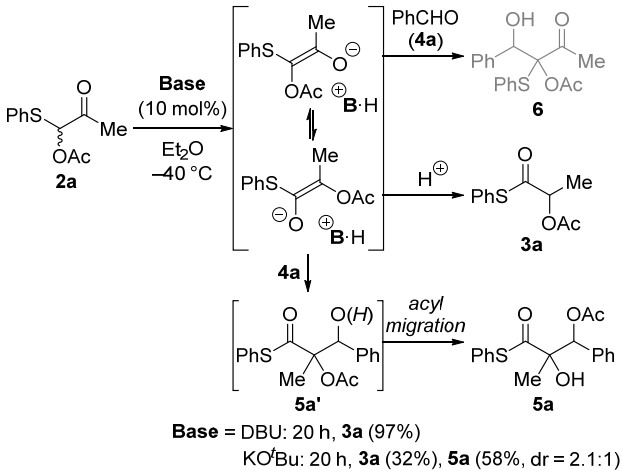

Scheme 1. Initial investigation of intrinsic reactivity of **2a**.

Table 1. Optimization of Reaction Conditions[a]

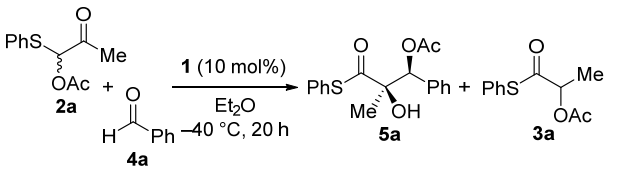

entry	1	yield (%)[b]	5a/3a[c]	dr[c]	ee (%)[d]
1	**1a**	90	12:1	13:1	6
2	**1b**	51	1:1	15:1	55
3	**1c**	76	4:1	12:1	70
4	**1d**	95	>20:1	20:1	87
5	**1e**	87	>20:1	18:1	92
6	**1f**	99	>20:1	>20:1	91
7	**1g**	90	>20:1	>20:1	92

[a] Reactions were performed with 0.1 mmol of **2a** and 0.11 mmol of **4a** in Et_2O (1.0 mL) in the presence of **1** (10 mol%) at −40 °C. [b] Isolated yield of a diastereomeric mixture of **5a**. [c] Ratios of products and diastereomers were determined by ^{1}H NMR (400 MHz) analysis of crude aliquot. [d] Absolute configuration of major diastereomer of **5a** was determined by X-ray crystallographic analysis (Figure 3).[16] Enantiomeric excesses of major diastereomer of **5a** were indicated, which were determined by using chiral stationary phase HPLC with Daicel CHIRALPAK AD-3 (hexane/2-propanol/EtOH = 45:4:1 as eluent).

conditions, smooth consumption of **2a** was observed within 20 h, resulting in the predominant formation of **5a** together with the protonation product **3a** (**5a**:**3a** = 12:1) (Table 1, entry 1). This result primarily suggests the importance of not only the pK_a value but also the structure of the base catalyst in diverting reactivity of the enediolate from the protonation to the aldol-acyl migration sequence. Although **5a** was obtained with relatively high diastereoselectivity (dr = 13:1), the enantiomeric excess of the major isomer was determined to be only 6%. We therefore pursued modification of the iminophosphorane structure to examine the effect on the selectivity profile; this revealed that the structural features of the alkyl substituent (R) constitute a critical element for modulating the ability of **1** to dictate the reaction pathway and the stereochemical outcome.

Switching the isopropyl moiety in **1a** to α-non-branched alkyl groups, such as methyl (**1b**) and isobutyl (**1c**), delivered an appreciable level of enantioselectivity, but the product distribution showed substantial participation of the undesired protonation (entries 2 and 3). In marked contrast, an increase in the steric bulkiness of the α-branched alkyl group from isopropyl to (*S*)-*sec*-butyl (**1d**) or cyclohexyl (**1e**) turned out to be beneficial for completely suppressing the formation of **3a**, while significantly improving the stereoselectivity (entries 4 and 5).[14] Further tuning of the properties of the aromatic appendage (Ar) enabled the identification of L-cyclohexylglycine-derived iminophosphorane **1g** bearing 4-fluorophenyl groups as an optimal catalyst, and **5a** was solely isolated as a single diastereomer (dr = >20:1) with high enantiomeric excess (92%) (entries 6 and 7).[15] The three-dimensional structure of **5a** was determined by single-crystal X-ray diffraction analysis to confirm the relative and absolute stereochemistry and regiochemistry at the carbon-carbon bond-forming event (Figure 3).[16]

With the optimized iminophosphorane catalyst in hand, further experiments were conducted to explore the scope and limitation of this new glycolate aldol protocol (Table 2). As the electrophilic component, a series of aromatic aldehydes **4** were employable regardless of their steric and electronic attributes (entries 1–10). However, when a strongly electron-withdrawing group such as methoxycarbonyl group was introduced to the *para*-position of the aromatic ring, lowering the reaction temperature was necessary to attain a synthetically satisfactory level of enantioselectivity, while virtually complete control of the reaction pathway and relative stereochemistry was consistently achievable (entry 4). 2-Naphthaldehyde and heteroaromatic aldehydes were also amenable to this catalytic system (entries 11–14). Although (*E*)-cinnamaldehyde could be accommodated by conducting the aldolization at lower

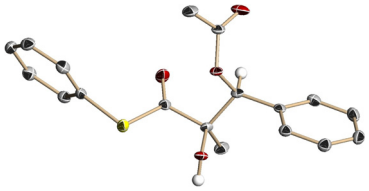

Figure 3. ORTEP diagram of **5a** (Ellipsoids displayed at 50% probability. Calculated hydrogen atoms except for them attached to the stereogenic carbon are omitted for clarity. Gray: carbon, red: oxygen, yellow: sulfur.).

Table 2. Substrate Scope and Limitation[a]

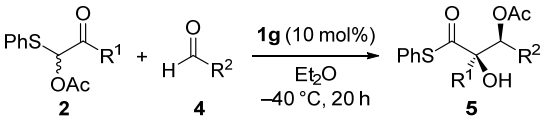

entry	R^1 (**2**)	R^2 (**4**)	yield (%)[b]	dr[c]	ee (%)[d]	**prod.**
1	Me (**2a**)	4-MeC_6H_4 (**4b**)	90	>20:1	92	**5b**
2	Me (**2a**)	4-ClC_6H_4 (**4c**)	94	>20:1	92	**5c**
3	Me (**2a**)	4-BrC_6H_4 (**4d**)	98	>20:1	92	**5d**
4[e,f]	Me (**2a**)	4-(MeOCO)C_6H_4 (**4e**)	83	>20:1	85	**5e**
5	Me (**2a**)	3-MeC_6H_4 (**4f**)	95	>20:1	92	**5f**
6	Me (**2a**)	3-$MeOC_6H_4$ (**4g**)	94	>20:1	94	**5g**
7	Me (**2a**)	3-FC_6H_4 (**4h**)	94	>20:1	84	**5h**
8	Me (**2a**)	2-MeC_6H_4 (**4i**)	74	>20:1	93	**5i**
9	Me (**2a**)	2-$MeOC_6H_4$ (**4j**)	88	>20:1	96	**5j**
10	Me (**2a**)	3,4-$(CH_2O_2)C_6H_3$ (**4k**)	90	12:1	95	**5k**
11	Me (**2a**)	2-Naphthyl (**4l**)	98	>20:1	93	**5l**
12	Me (**2a**)	3-furyl (**4m**)	88	>20:1	93	**5m**
13	Me (**2a**)	3-thienyl (**4n**)	95	>20:1	91	**5n**
14	Me (**2a**)	2-thienyl (**4o**)	96	>20:1	86	**5o**
15[e,g]	Me (**2a**)	(*E*)-PhCH=CH (**4p**)	95	20:1	83	**5p**
16[h]	Me (**2a**)	$Ph(CH_2)_2$ (**4q**)	66	10:1	37	**5q**
17[h]	Et (**2b**)	Ph (**4a**)	80	14:1	97	**5r**
18	$MeOCH_2$ (**2c**)	Ph (**4a**)	73	17:1	87	**5s**
19[e,f]	$Me(CH_2)_3$ (**2d**)	Ph (**4a**)	68	6.7:1	94	**5t**
20	(*E*)-MeCH=CH (**2e**)	Ph (**4a**)	79	1.5:1	92[i]	**5u**

[a] Unless otherwise noted, reactions were conducted with 0.1 mmol of **2** and 0.11 mmol of **4** in Et_2O (1.0 mL) in the presence of **1g** (10 mol%) at −40 °C for 20 h. [b] Isolated yield of a mixture of diastereomers was indicated. [c] Diastereomeric ratios were determined by ^1H NMR (400 MHz) analysis of crude aliquot. [d] Absolute configuration of **5** was assigned by analogy of **5a**. Enantiomeric excesses of the major diastereomer were indicated, which were analyzed by chiral stationary phase HPLC. [e] Reaction was conducted at −60 °C. [f] Reaction time was 96 h. [g] Reaction time was 72 h. [h] Reaction time was 48 h. [i] Enantiomeric excess of the minor diastereomer was 25%.

temperature, considerable decrease in stereoselectivity was inevitable in the coupling with an aliphatic aldehyde (entries 15 and 16). With respect to the nucleophile **2**, variation in the acyl substituent appeared feasible, albeit with a slight decrease in the efficiency and stereocontrol (entries 17–19). It should be added that the loss in diastereoselectivity was significant in the reaction of α-acetoxy-β-ketosulfide having an enone moiety (entry 20).

As illustrated in Scheme 2, treatment of the product **5a** with

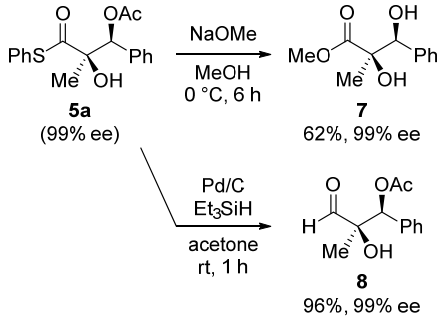

Scheme 2. Conversion of **5a** to α,β-dihydroxy ester **7** and α-hydroxy aldehyde **8**.

sodium methoxide at 0 °C facilitated smooth double transesterification of the thioester moiety and the acetyl unit to afford α,β-dihydroxy ester **7** in good yield. This simple derivatization demonstrates the immediate utility of the present method as a reliable tool for straightforward access to stereochemically homogeneous α,β-dihydroxycarboxylic acids and their derivatives possessing a fully substituted stereocenter at the α-carbon atom, which are often encountered as partial structures of biologically active natural products and also serve as valuable chiral synthons. By further taking advantage of the thioester moiety that is known to be easily converted into other carbonyl functionalities, **5a** could be effectively reduced by the Fukuyama's procedure into the α-hydroxy aldehyde **8** without loss of the stereochemical integrity.[17]

To gain insight into the origin of the catalyst-directed multiple selectivity control, particularly the precise dictation of the reaction pathway, we performed DFT calculations (Gaussian 09)[18] for analyzing the reaction of the realistic substrate set, α-acetoxy-β-ketosulfide **2a** and benzaldehyde (**4a**), with iminophosphorane **1e** as a catalyst (entry 5 in Table 1).[7k,19] Geometries of the intermediates and transition states were fully optimized and characterized by frequency calculations at the PCM(Et_2O)-ωB97XD/6-31G(d,p) level. Single-point energies of the optimized structures at the PCM(Et_2O)-ωB97XD/6-311++G(d,p) level were calculated and combined with the thermal corrections estimated by PCM(Et_2O)-ωB97XD/6-31G(d,p) to obtain Gibbs free energies (ΔG). The calculated Gibbs free energy profile (233.15 K, 1 atm) is displayed in Figure 4.

First, deprotonation of racemic **2a** with **1e** generates the corresponding aminophosphonium enediolate **1e**·H·[**2a**–H] (**Enol1-E**), where **1e**·H featuring two N-H protons captures [**2a**–H]$^-$ in a way that one N-H proton makes a hydrogen bond with the anionic enolate oxygen and the other with the acetate carbonyl. This deprotonation proceeds via the relatively high-energy transition state (TS) **TS-PT1-RE** (from (*R*)-**2a**) and **TS-PT1-SE** (from (*S*)-**2a**) (+6.9 and +9.1 kcal·mol^{-1}, respectively).

The **Enol1-E** thus generated could potentially participate in the three different reactions, namely (i) re-protonation at C1 to liberate the parent **2a** and the catalyst **1e** (**TS-PT1-RE**), (ii) aldol reaction with **4a** via **TS-CC1-SS**,[20] and (iii) intramolecular acyl migration to give the putative cyclic enediolate **INT-Cyc1** via **TS-Cyc1**. Optimization of the structures and calculation of Gibbs free energies of appropriate TS models for these reaction courses confirmed that the acyl migration was the most favorable pathway as **TS-Cyc1** has the lowest free energy (+5.9 kcal·mol^{-1}). This outcome reflects the higher energy estimated for the TS for the C-C bond formation,

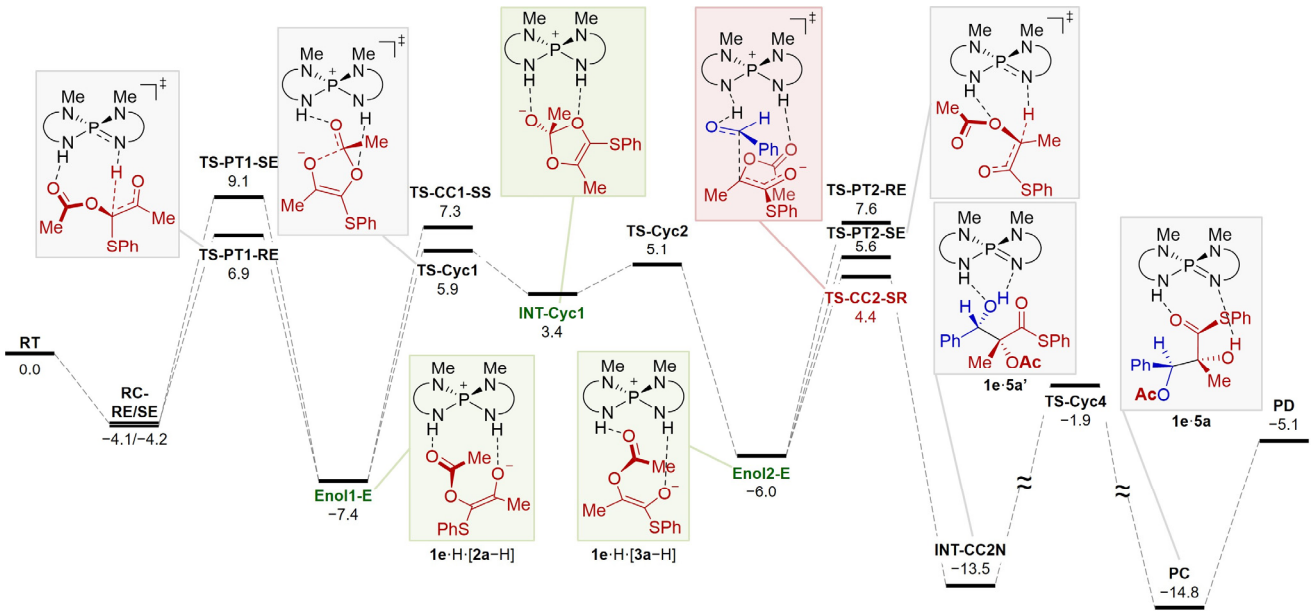

Figure 4. Gibbs free energy profile of the reaction at PCM(Et_2O)-ωB97XD/6-311++G(d,p)//PCM(Et_2O)-ωB97XD/6-31G(d,p). Gibbs free energies relative to **RT** are in kcal·mol^{-1} (233.15 K, 1 atm). **RT** = reactant, **RC** = reactant complex, **PC** = product complex, **PD** = product.

TS-CC1-SS, which is in accord with the experimental observation that the aldol reaction from **Enol1-E** did not take place regardless of the base catalyst employed likely due to the innate instability of the product ion pair.[21]

The resulting **INT-Cyc1** either leads to generate another aminophosphonium enediolate **1e**·H·[**3a**–H] (**Enol2-E**) via **TS-Cyc2** or goes back to **Enol1-E**. Judging from the relatively low energy barriers in the acyl migration processes, the two aminophosphonium enediolates, **Enol1-E** and **Enol2-E**, would equilibrate slowly through the intermediacy of **INT-Cyc1**, although the equilibrium is largely inclined toward **Enol1-E**. The transient **INT-Cyc1** lies higher in energy and would have low probability of being present. In fact, a TS model for the C-C bond formation from **INT-Cyc1** could not be located.

Interestingly, the TS for the aminophosphonium enediolate **Enol2-E** to engage in the aldolization with **4a** (**TS-CC2-SR**) has a lower free energy (+4.4 kcal·mol^{-1}) than that of the TS for the reverse acyl migration (**TS-Cyc2**), thus rendering this C-C bond formation pathway predominant. It is worthy of note that, upon forming **TS-CC2-SR**, the aminophosphonium ion **1e**·H releases the anionic enolate oxygen of [**3a**–H]$^-$, rather than the carbonyl oxygen, through the disruption of the hydrogen bond and incorporates **4a** using the resultant free N-H proton as visualized by the three-dimensional representation in Figure 5a.[22] Compared to another possible TS that retains the hydrogen bonding from the N-H proton to the anionic oxygen (**TS-CC2-SR'**, Figure 5b), **4a** is aligned as to enjoy CH-π interaction between the phenyl group and one of the cyclohexyl

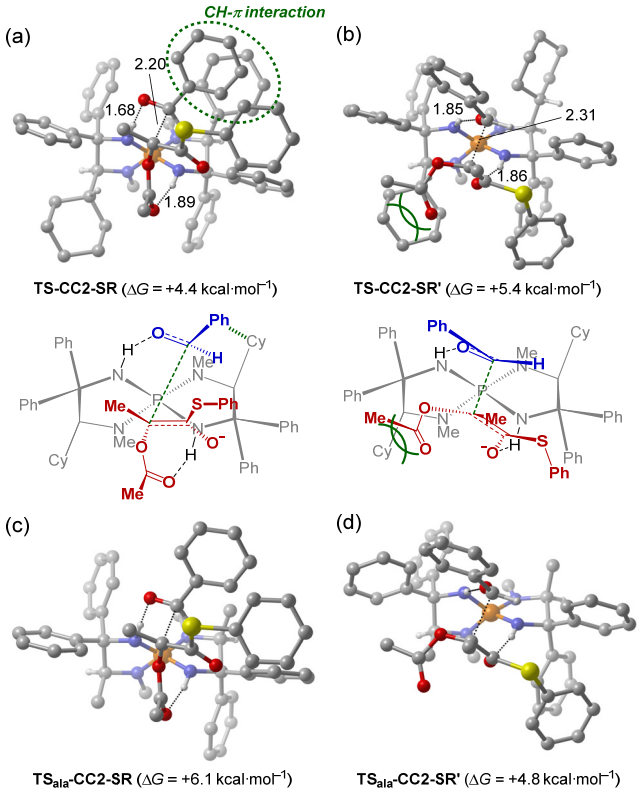

Figure 5. Three dimensional structures and Gibbs free energies relative to **RT** (233.15 K, 1 atm) in TSs for C-C-bond formation in **1e**- and **1b**-catalyzed reactions. (a) **TS-CC2-SR**, (b) **TS-CC2-SR'**, (c) **TS$_{ala}$-CC2-SR**, (d) **TS$_{ala}$-CC2-SR'**. Interatomic distances are in Å. Unimportant hydrogen atoms are omitted for clarity.

substituents of **1e**·H (highlighted in green dotted circle), and the steric repulsion between the acetate moiety and the other cyclohexyl substituent is relieved. Moreover, the SPh moiety of [**3a**–H]$^-$ is disposed outside the chiral cavity of **1e**·H and is liberated from any steric constraints. The interplay of the attractive CH-π interaction and the favorable steric effects compensates the destabilization caused by the loss of otherwise preferable hydrogen-bonding interaction to stabilize the enolate anion, which contributes to the small energy barrier calculated for the aldolization via **TS-CC2-SR**.

In addition, the high energy barrier calculated for the protonation of [**3a**–H]$^-$ by the pairing **1e**·H is crucial for **1e**·H to guide [**3a**–H]$^-$ toward intermolecular aldol coupling.[23] The instability of the TSs for the protonation at the C-2 position of [**3a**–H]$^-$ (**TS-PT2-SE** and **TS-PT2-RE**) could be attributed to the structural feature of **1e**·H bearing cyclohexyl substituents. The steric hindrance of the cyclohexyl groups allows **1e**·H to exploit a significant repulsive nonbonding interaction with [**3a**–H]$^-$ in restraining the formation of **TS-PT2-SE** and **TS-PT2-RE**; this raises the energy barrier for [**3a**–H]$^-$ to undergo protonation to yield **3a** (+5.6 and +7.6 kcal·mol^{-1} for *S*- and *R*-**3a**, respectively), exceeding the free energy of **TS-CC2-SR** for the C-C bond formation process.

The critical importance of the cyclohexyl substituents of **1e**·H in overturning the inherent reactivity preference of the enediolate [**3a**–H]$^-$ was also corroborated by delineating the free energy profile of the reaction with the L-alanine-derived iminophosphorane **1b** possessing methyl substituents as a catalyst. The calculated Gibbs free energy of the analogous TS for the **1b**-catalyzed aldolization giving *SR*-**5a** (**TS$_{ala}$-CC2-SR**) was higher than that of **TS-CC2-SR** mainly due to the lack of the CH-π interaction (Figure 5a vs 5c). Rather, another TS, **TS$_{ala}$-CC2-SR'** (Figure 5d), where one N-H proton of **1b**·H interacts with the anionic oxygen of [**3a**–H]$^-$, lies lower in energy (+4.8 kcal·mol^{-1}), suggesting that no particular steric repulsion between the acetate moiety of [**3a**–H]$^-$ and one methyl substituent of **1b**·H allows to appreciate the stabilization of the enolate anion by the hydrogen-bonding interaction (Figure 5b vs 5d). Furthermore, the sterically less demanding **1b**·H is also able to form a slightly tighter ion pair with [**3a**–H]$^-$ without being interfered with notable collisions, lowering the free energy of the TS for protonation (**TS$_{ala}$-PT2-RE**: +5.1 kcal·mol^{-1});[21] this makes the free energy difference between **TS$_{ala}$-CC2-SR'** and **TS$_{ala}$-PT2-RE** small enough for both processes to occur in a comparable rate as experimentally observed (see Table 1, entry 2).

Having grasped a detailed picture of how the iminophosphorane catalyst guides the sulfur-substituted enediolate toward the aldol reaction, we next compared the Gibbs free energies of the possible diastereomeric TS models for the **1e**-catalyzed aldolization of **2a** with **4a** to understand the stereoselectivity profile (Figure 6). While the energy values calculated at the PCM(Et_2O)-ωB97XD/6-311++G(d,p)//PCM(Et_2O)-ωB97XD/6-31G(d,p) level (233.15 K, 1 atm) successfully predicted that **TS-CC2-SR** giving the experimentally obtained major stereoisomer was the most stable TS, the free energy differences (ΔΔG) between other diastereomeric TSs were not well correlated with the observed diastereo- and enantioselectivity. Therefore, in order to improve the quantitative reproducibility in stereoselectivity, we conducted single point calculations on these TSs using the M06-2X functional known to be suitable for analyzing aldol

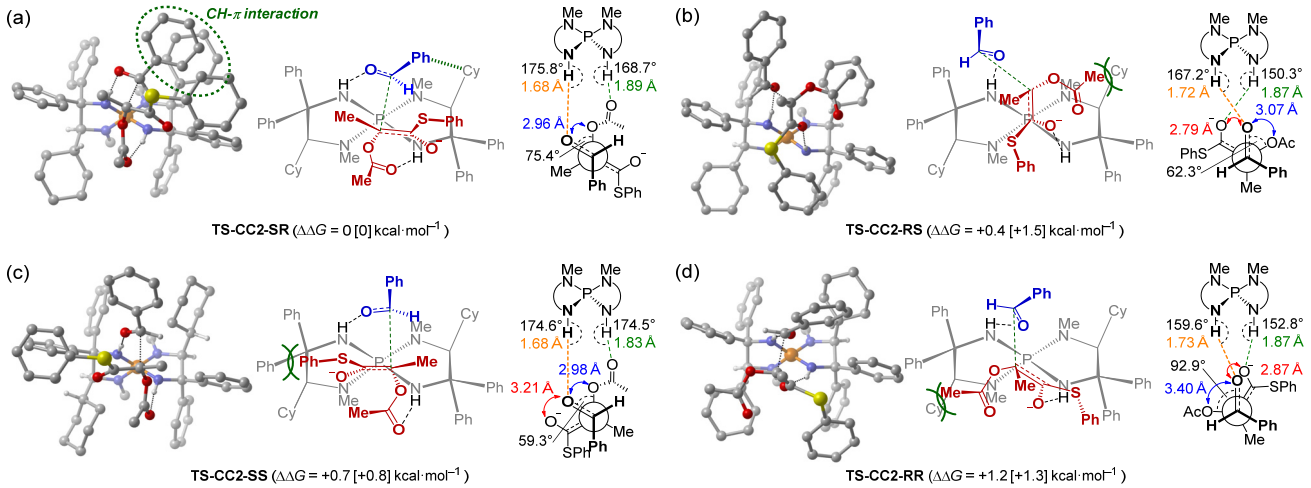

(e)

	ΔE_{dis} (kcal·mol^{-1})		ΔE_{int}	ΔE_{sol}	ΔE_{tot} (ΔE_{dis}+ΔE_{int}+ΔE_{sol})
	sub	cat	(kcal·mol^{-1})	(kcal·mol^{-1})	(kcal·mol^{-1})
SR	0.0	0.0	0.0	0.0	0.0
RS	+7.5	+3.6	−10.7	+0.5	+0.9
SS	+5.9	−0.2	−2.8	−0.6	+2.3
RR	+9.4	+3.6	−11.7	+0.5	+1.9

Figure 6. (a)~(d) TS-models leading possible four diastereomers at the aldolization. Gibbs free energies relative to **TS-CC2-SR** are in kcal·mol^{-1} (233.15 K, 1 atm) at PCM(Et_2O)-ωB97XD/6-311++G(d,p)//PCM(Et_2O)-ωB97XD/6-31G(d,p) [PCM(Et_2O)-M06-2X/6-311++G(d,p)//PCM(Et_2O)-ωB97XD/6-31G(d,p)]. Unimportant hydrogen atoms are omitted for clarity. (e) Distortion/interaction analysis on diastereomeric **TS-CC2** structures at M06-2X/6-311++G(d,p)//PCM(Et_2O)-ωB97XD/6-31G(d,p).

reactions (indicated in square brackets).[24] As a result, the derived energy difference between **TS-CC2-SR** and **TS-CC2-RS** (ΔΔG = +1.5 kcal·mol^{-1}) was in good agreement with the experimentally observed enantioselectivity, but the difference between **TS-CC2-SR** and **TS-CC2-SS** (ΔΔG = +0.8 kcal·mol^{-1}) was not sufficiently large to rationalize the observed diastereoselectivity.

Since the calculations at M06-2X/6-311++G(d,p) qualitatively accounted for the stereoselectivity of the C-C bond formation, we investigated the origin of the obtained energy differences by applying the distortion/interaction analysis to the diastereomeric TSs. The relative distortion (ΔE_{dis}) and interaction (ΔE_{int}) energies with respect to the values in **TS-CC2-SR** are summarized in Figure 6e. In **TS-CC2-RR** and **TS-CC2-RS**, a large positive ΔE_{dis} (+13.0 and +11.1 kcal·mol^{-1}) and negative ΔE_{int} (− 11.7 and − 10.7 kcal·mol^{-1}) were recognized, where ΔE_{dis} of the substrate was much larger than that of the catalyst. On the other hand, **TS-CC2-SS** showed a moderate positive ΔE_{dis} of the substrate (+5.9 kcal·mol^{-1}) and a small negative ΔE_{int} (− 2.8 kcal·mol^{-1}). The significant differences of ΔE_{dis} of the substrate in these three TSs from that in **TS-CC2-SR** could originate from the electrostatic repulsion between the oxygen atoms in the approaching substrates (see Newman projections in Figure 6). Specifically, the oxygen atom of **4a**, on which a negative charge is developed along with the formation of a new C-C bond, is oriented *gauche* to both the acetate and the thioester enolate components of the enediolate [**3a**−H]$^-$. Only **TS-CC2-SR** is free from this issue given that the oxygen atom of **4a** adopts an *anti* relation to the negatively charged thioester enolate oxygen. In addition, the CH-π interaction between the phenyl group of **4a** and the cyclohexyl substituent of **1e**·H contributes to the stabilization of **TS-CC2-SR**, which is in accordance with the diminished stereoselectivity observed in the reaction with the aliphatic aldehyde (Table 2, entry 16). The large negative ΔE_{int} values in **TS-CC2-RR** and **TS-CC2-RS** clearly indicate that the hydrogen bond between the N-H proton of **1e**·H and the anionic oxygen of [**3a**−H]$^-$ is strongly favored. However, the catalyst must be distorted to incorporate the substrates for the intermolecular aldolization in a manner that the acetate moiety of [**3a**−H]$^-$ is placed close to one of the cyclohexyl substituents of **1e**·H (+3.6 kcal·mol^{-1}). Consequently, distortion energies slightly surpass the stabilization effect provided by the hydrogen-bonding interactions, resulting in the destabilization of **TS-CC2-RR** and **TS-CC2-RS**. In **TS-CC2-SS**, the mode of the hydrogen-bonding interactions was the same with that in **TS-CC2-SR** and they were even stronger as evident from the shorter H···O distance and more linear N-H···O angle of the hydrogen bonding to the acetate carbonyl of [**3a**−H]$^-$. Nevertheless, the interactions beneficial for gaining stabilization appear to be too small to override the influence of the distortion energy mainly arising from the proximity between the SPh moiety of [**3a**−H]$^-$ and one of the geminal phenyl substituents of **1e**·H, rendering **TS-CC2-SS** unstable.

The C-C bond-forming event accompanied by the asynchronous proton transfer from **1e**·H afforded a neutral complex **1e**·**5a'** (**INT-CC2N**). Subsequently, **INT-CC2N** was converted into a stable complex of **1e** with **5a** (**PC**) through multiple processes, including intramolecular acyl migration.[19] **PC** would liberate the aldol product with the concomitant regeneration of the iminophosphorane **1e**, closing the entire catalytic cycle.

CONCLUSIONS

We demonstrated that sulfur-substituted enediolates, generated in situ from α-acylated hemithioacetals **2**, selectively engaged in the glycolate aldol reaction with aldehydes **4** with an excellent level of diastereo- and enantiocontrol under the

catalysis of the L-cyclohexylglycine-derived chiral iminophosphorane **1g**. While the pK_a balance in the intermediary formed aminophosphonium enediolate **1**·H·[**3**−H] would urge a pseudo-intramolecular proton transfer to liberate **1** and α-hydroxy thioester **3**, the intermolecular carbon-carbon bond formation proceeded predominantly over the protonation in a highly stereoselective manner when **1g** was employed as a catalyst. The unique and relevant features of **1g** for precisely dictating the reaction pathway and the stereochemical outcome were dissected by extensive quantum analysis, revealing the critical importance of cyclohexyl substituents in the simultaneous control of the multiple selectivities. These results shed light on the previously unexplored possibility of utilizing the base-catalyzed hemithioacetal isomerization as a tool for the generation of highly basic enolates by the judicious choice of a catalyst capable of kinetically suppressing the rapid protonation and directing the subsequent stereoselective bond-forming reactions. This significant implication will stimulate the development of new catalyst-controlled strategies for achieving otherwise difficult transformations under simple acid-base catalysis.

ASSOCIATED CONTENT

*Supporting Information

The Supporting Informations are available free of charge on the ACS Publications website at DOI: 10.1021/jacs.0000000.

Experiment details, spectral data, copies of ^{1}H and ^{13}C NMR spectra, and copies of HPLC traces (PDF)

Computational details and discussion (PDF).

Cartesian coordinates and energies (PDF).

X-ray crystallographic data for **1e**·HCl and **5a** (CIF)

AUTHOR INFORMATION

Corresponding Author

*tooi@chembio.nagoya-u.ac.jp

ORCID

Takashi Ooi: 0000-0003-2332-0472

Daisuke Uraguchi: 0000-0002-6584-797X

Makoto Sato: 0000-0001-8903-6226

Notes

The authors declare no competing financial interest.

ACKNOWLEDGMENT

Financial support was provided by CREST-JST (JPMJCR13L2: 13418441), Program for Leading Graduate Schools "Integrative Graduate Education and Research Program in Green Natural Sciences" in Nagoya University, and Grants of JSPS for Scientific Research. KY acknowledges JSPS for financial support. The computations were performed using Research Center for Computational Science, Okazaki, Japan.

REFERENCES

(1) (a) Hall, S. S.; Doweyko, A. M.; Jordan, F. *J. Am. Chem. Soc.* **1976**, *98*, 7460–7461. (b) Hall, S. S.; Doweyko, A. M.; Jordan, F. *J. Am. Chem. Soc.* **1978**, *100*, 5934–5939. (c) Shinkai, S.; Yamashita, T.; Kusano, Y.; Manabe, O. *Chem. Lett.* **1979**, 1323–1326. (d) Shinkai, S.; Yamashita, T.; Kusano, Y.; Manabe, O. *J. Am. Chem. Soc.* **1981**, *103*, 2070–2074. (e) Landro, J. A.; Brush, E. J.; Kozarich, J. W. *Biochemistry* **1992**, *31*, 6069–6077. (f) Ridderström, M.; Cameron, A. D.; Jones, T. A.; Mannervik, B. *J. Biol. Chem.* **1998**, *273*, 21623–21628. (g) Thornalley, P. J. *Biochem. Soc. Trans.* **2003**, *31*, 1343–1348.

(2) (a) Schmitt, E.; Schiffers, I.; Bolm, C. *Tetrahedron Lett.* **2009**, *50*, 3185–3188. (b) Park, S. Y.; Hwang, I.-S.; Lee, H.-J.; Song, C. E. *Nat. Commun.* **2017**, *8*, 14877.

(3) (a) de Lucchi, O.; Miotti, U.; Modena, G. *Org. React.* **1991**, *40*, 157–405. (b) Padwa, A.; Gunn, Jr., D. E.; Osterhout, M. H. *Synthesis* **1997**, 1353–1377. (c) Padwa, A.; Bur, S. K.; Danca, D. M.; Ginn, J. D.; Lynch, S. M. *Synlett* **2002**, 851–862. (d) Bur, S. K.; Padwa, A. *Chem. Rev.* **2004**, *104*, 2401–2432.

(4) (a) Iriuchijima, S.; Maniwa, K.; Tsuchihashi, G.-I. *J. Am. Chem. Soc.* **1975**, *97*, 596–599. (b) Russell, G. A.; Mikol, G. J. *J. Am. Chem. Soc.* **1966**, *88*, 5498–5504. (c) Capitta, F.; Melis, N.; Secci, F.; Romanazzi, G.; Frongia, A. *J. Sulfur Chem.* **2014**, *35*, 649–660.

(5) (a) Mimoto, T.; Terashima, K.; Nojima, S.; Takaku, H.; Nakayama, M.; Shintani, M.; Yamaoka, T.; Hayashi, H. *Bioorg. Med. Chem.* **2004**, *12*, 281–293. (b) Suzuki, T.; Honda, Y.; Izawa, K.; Williams, R. M. *J. Org. Chem.* **2005**, *70*, 7317–7323. (c) Capitta, F.; Frongia, A.; Piras, P. P.; Pitzanti, P. *Adv. Synth. Catal.* **2010**, *352*, 2955–2960.

(6) (a) Corbett, M. T.; Uraguchi, D.; Ooi, T.; Johnson, J. S. *Angew. Chem. Int. Ed.* **2012**, *51*, 4685–4689. (b) Horwitz, M. A.; Tanaka, N.; Yokosaka, T.; Uraguchi, D.; Johnson, J. S.; Ooi, T. *Chem. Sci.* **2015**, *6*, 6086–6090.

(7) (a) Uraguchi, D.; Ooi, T. *J. Synth. Org. Chem. Jpn.* **2010**, *68*, 1185–1194. (b) Uraguchi, D.; Nakamura, S.; Ooi, T. *Angew. Chem. Int. Ed.* **2010**, *49*, 7562–7565. (c) Uraguchi, D.; Yoshioka, K.; Ueki, Y.; Ooi, T. *J. Am. Chem. Soc.* **2012**, *134*, 19370–19373. (d) Uraguchi, D.; Tsutsumi, R.; Ooi, T. *J. Am. Chem. Soc.* **2013**, *135*, 8161–8164. (e) Uraguchi, D.; Yamada, K.; Ooi, T. *Angew. Chem. Int. Ed.* **2015**, *54*, 9954–9957. (f) Uraguchi, D.; Yoshioka, K.; Ooi, T. *Nat. Commun.* **2017**, *8*, 14793. (g) Uraguchi, D.; Ito, T.; Kimura, Y.; Nobori, Y.; Sato, M.; Ooi, T. *Bull. Chem. Soc. Jpn.* **2017**, *90*, 546–555. (h) Yoshioka, K.; Yamada, K.; Uraguchi, D.; Ooi, T. *Chem. Commun.* **2017**, *53*, 5495–5498. (i) Tanaka, N.; Tsutsumi, R.; Uraguchi, D.; Ooi, T. *Chem. Commun.* **2017**, *53*, 6999–7002. (j) Uraguchi, D.; Kawai, Y.; Sasaki, H.; Yamada, K.; Ooi, T. *Chem. Lett.* **2018**, *47*, doi: 10.1246/cl.180031. (k) Uraguchi, D.; Shibazaki, R.; Tanaka, N.; Yamada, K.; Yoshioka, K.; Ooi, T. *Angew. Chem. Int. Ed.* **2018**, *57*, doi: 10.1002/anie.201800057.

(8) For a review on organic base catalysis, see: Palomo, C.; Oiarbide, M.; López, R. *Chem. Soc. Rev.* **2009**, *38*, 632–653.

(9) For reviews on phosphonium salt catalyses, see: (a) Werner, T. *Adv. Synth. Catal.* **2009**, *351*, 1469–1481. (b) Enders, D.; Nguyen, T. V. *Org. Biomol. Chem.* **2012**, *10*, 5327–5331.

(10) Triaminoiminophosphoranes are known as a P1-phosphazenes, which was developed by Schwesinger, see: (a) Schwesinger, R.; Schlemper, H. *Angew. Chem. Int. Ed. Engl.* **1987**, *26*, 1167–1169. For a review, see: (b) Ishikawa, T. *Superbases for Organic Synthesis: Guanidines, Amidines, Phosphazenes and Related Organocatalysts*; John Wiley & Sons: West Sussex, U.K., 2009.

(11) For a review on chiral iminophosphorane catalysis, see: Krawczyk, H.; Dzięgielewski, M.; Deredas, D.; Albrecht, A.; Albrecht, Ł. *Chem. Eur. J.* **2015**, *21*, 10268–10277.

(12) (a) Takeda, T.; Terada, M. *J. Am. Chem. Soc.* **2013**, *135*, 15306–15309. (b) Núñez, M. G.; Farley, A. J. M.; Dixon, D. J. *J. Am. Chem. Soc.* **2013**, *135*, 16348–16351. (c) Gao, X.; Han, J.; Wang, L. *Org. Lett.* **2015**, *17*, 4596–4599. (d) Kondoh, A.; Oishi, M.; Takeda, T.; Terada, M. *Angew. Chem. Int. Ed.* **2015**, *54*, 15836–15839. (e) Farley, A. J. M.; Sandford, C.; Dixon, D. J. *J. Am. Chem. Soc.* **2015**, *137*, 15992–15995. (f) Robertson, G. P.; Farley, A. J. M.; Dixon, D. J. *Synlett* **2016**, *27*, 21–24. (g) Horwitz, M. A.; Zavesky, B. P.; Martinez-Alvarado, J. I.; Johnson, J. S. *Org. Lett.* **2016**, *18*, 36–39. (h) Gao, X.; Han, J.; Wang, L. *Org. Chem. Front.* **2016**, *3*, 656–660. (i) Takeda, T.; Kondoh, A.; Terada, M. *Angew. Chem. Int. Ed.* **2016**, *55*, 4734–4737. (j) Yang, J.; Farley, A. J. M.; Dixon, D. J. *Chem. Sci.* **2017**, *8*, 606–610.

(13) The hydrochloric acid salt of **1a** (*P*-VIP·Cl) is commercially available from Wako pure chemical industries (Cat. No. 226-02381).

(14) Upon treatment of **3a** with 10 mol% of **1d** in the presence of **4a** in diethyl ether, neither formation of **5a** nor consumption of **3a** was detected even at 0 °C. This indicated that the observed rigorous chemoselectivity was kinetically established.

(15) When the **1g**-catalyzed reaction was quenched after 2 h (37% conversion), enantiomerically enriched **2a** (15% ee) was recovered.

(16) Crystallographic data (excluding structure factors) for the structure reported in this paper have been deposited with the Cambridge Crystallographic Data Centre as supplementary publication no. CCDC 1588205 (**5a**) and CCDC 1588206 (**1g**·HCl). Copies of the data can be obtained free of charge on application to CCDC, 12 Union Road, Cambridge CB2 1EZ, UK (fax: (+44) 1223-336-033; e-mail: deposit@ccdc.cam.ac.uk).

(17) (a) Fukuyama, T.; Lin, S.-C.; Li, L. *J. Am. Chem. Soc.* **1990**, *112*, 7050–7051. (b) Tokuyama, H.; Yokoshima, S.; Lin, S.-C.; Li, L.; Fukuyama, T. *Synthesis* **2002**, 1121–1123.

(18) Gaussian 09, Revision D.01., Frisch, M. J. et al. Gaussian, Inc.: Wallingford, CT, 2013.

(19) Computational analysis on *P*-spiro chiral iminophosphorane catalysis, see: (a) Simón, L.; Paton, R. S. *J. Org. Chem.* **2015**, *80*, 2756–2766. (b) Yamanaka, M.; Sakata, K.; Yoshioka, K.; Uraguchi, D.; Ooi, T. *J. Org. Chem.* **2017**, *82*, 541–548. (c) Simón, L.; Paton, R. S. *J. Org. Chem.* **2017**, *82*, 3855–3863.

(20) See the Computational Supporting Information (CSI) for other TSs having higher energy.

(21) See CSI for details.

(22) CYLview, 1.0b, Legault, C. Y. Université de Sherbrooke, 2009.

(23) When the reaction was conducted in the presence of MS4A, essentially the same result was obtained, indicating that protonation of [**3a**−H]$^-$ with water molecule is unlikely. While proton delivery from either **2a** or **3a** is another possible scenario, intervention of this process would also be negligible because the protonation/aldolization ratio was found to be insensitive to the reaction concentration and optimized TSs for such protonation of [**3a**−H]$^-$ have higher energy than that of **TS-PT2-SE** (See S34 in CSI).

(24) (a) Um, J. M.; Gutierrez, O.; Schoenebeck, F.; Houk, K. N.; MacMillan, D. W. C. *J. Am. Chem. Soc.* **2010**, *132*, 6001–6005. (b) Grayson, M. N.; Houk, K. N. *J. Am. Chem. Soc.* **2016**, *138*, 9041–9044.

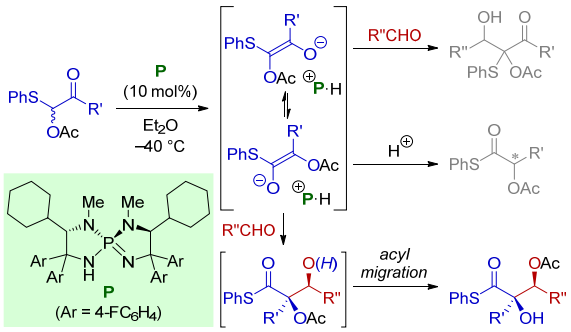
PhS
R'
OAc
O
P
(10 mol%)
Et2O
–40 °C
P·H
R"CHO
OH
R''
PhS
OAc
H
acyl
migration
Me
N
P
Ar
H
(Ar = 4-FC6H4)